ATMOSPHERIC ENTRY SIMULATION OF CHONDRITIC MATERIALS AND LINKS TO MICROMETEORITES

H5 OC HaH 077

Abstract [#6256]

84th Annual Meeting of the Meteoritical Society Chicago

C. E. Kampf1,2, C. Hamann1, S. Schäffer3, D. Heunoske3, T. Hasse1, L. Hecht1,2, A. Greshake1, and J. Osterholz3,
1Museum für Naturkunde Berlin, Germany (clara.kampf@mfn.berlin),
2Institut f. Geologische Wissenschaften, Freie Universität Berlin, Germany, 3Fraunhofer-Institut für Kurzzeitdynamik, Ernst-Mach-Institut, Freiburg, Germany

Summary During atmospheric entry chondritic material experiences fragmentation, melting, evaporation, mass loss, metal-silicate segregation and changes in oxygen-fugacity (fO_2) conditions prior to the rapid quenching of the superheated melt. This typically generates fusion crusts coating the meteorites (e.g., [1,2]) as well as formation of micrometeorites, and induces significant changes in chemical and mineralogical compositions [2,5] associated with the flash heating during entry. Here, we present a comparison of laser-produced melts of the *H5 ordinary chondrite* Hammadah al Hamra (HaH) 077 against *natural fusion crusts* on ordinary chondrites [2] and a subset of *pristine micrometeorites* [6]. The results of this study attests to the adequacy of the experimental set up to successfully simulate atmospheric entry with the formation of a fusion crust and all its characteristic components and thus allows comparison of experimental materials against natural to establish a better understanding of the involved, intricate processes and their products, enableing unbiased interpretations.

Materials and Methods

We used a continuous-wave (CW) fiber laser with a wavelength of 1.07 µm at Fraunhofer Institut für Kurzzeitdynamik in Freiburg, Germany to irradiate a piece of H5 OC HaH 077 in ambient air at 1 bar and room temperature. Over periods of 5-10 s the CW fiber laser emitted with a power of 8 kW and an average intensity of 2.2 × 10^5 W/cm^2 onto the sample, with a beam diameter of 2 mm [7] (Fig.1). The laser excavated several sub-µm to mm sized melt spherules that were ejected ballistically onto witness plates in 1-3 cm distance. Thermal imaging by an infrared pyrometer suggests temperatures exceeding the detection limit, registering a 5 s plateau on 2100 °C prior to rapid cooling to room temperature within seconds after cessation of irradiation. Textural and compositional characterization of the laser-produced melts and the pristine set of urban micrometeorites employed field-emission scanning electron microscopy (SEM) and low-voltage energy dispersive spectroscopy (EDX) at the Imaging and Analysis Centre, Natural History Museum, London, UK, as well as at Museum für Naturkunde Berlin, Germany with additional field emission EMPA analysis with an electron microprobe. The sampling of the pristine urban micrometeorites from the rooftops and their thorough investigation and selection process is described in detail in [6].

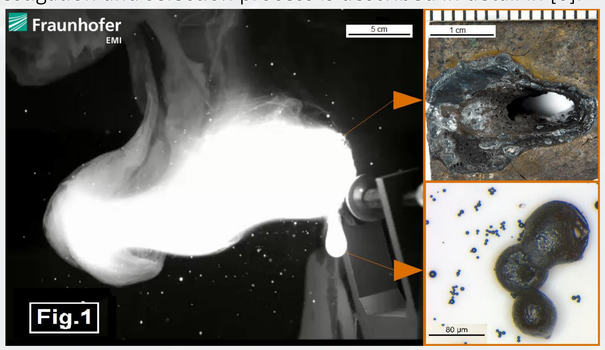

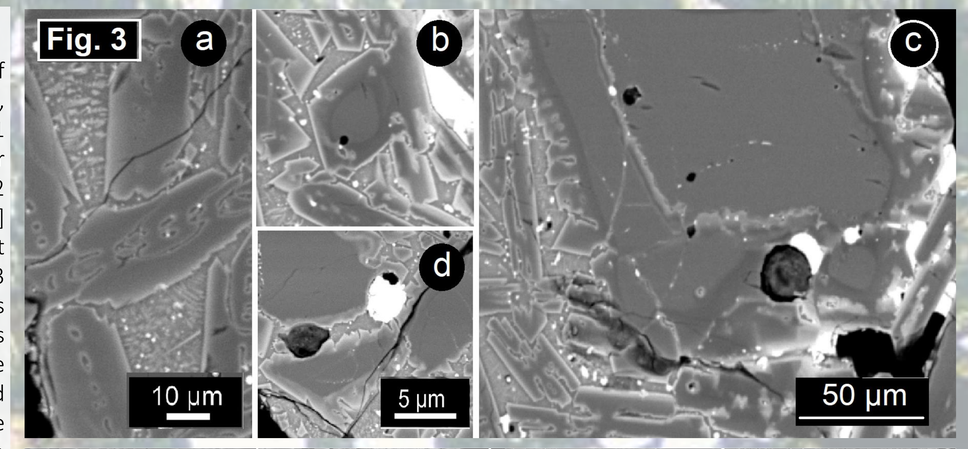

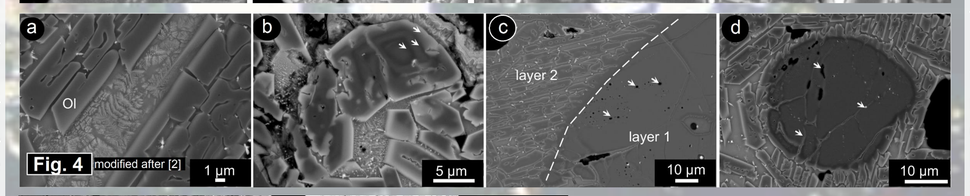

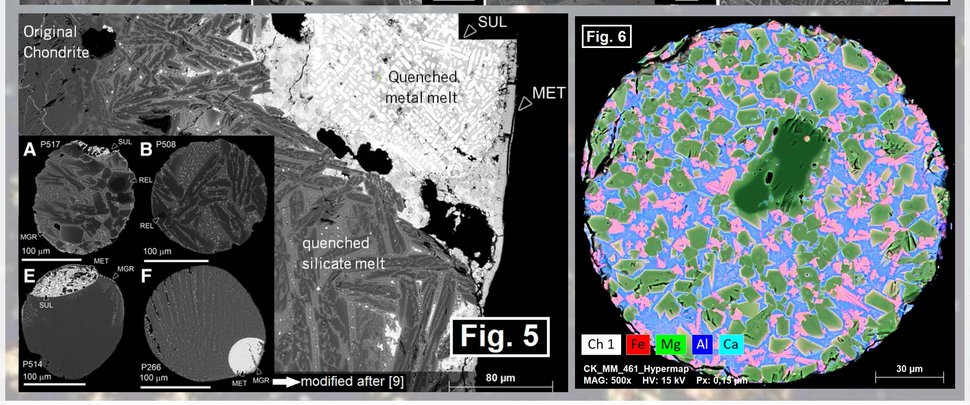

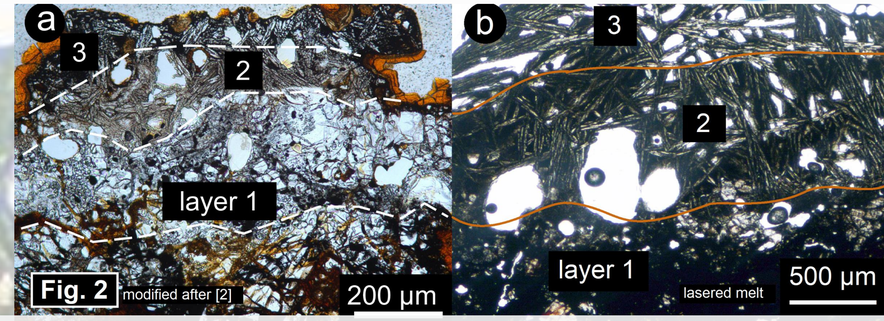

Petrographic observations

The natural fusion crust (Fig.2 a) compromises 3 layers that we were able to identify through evident similarities in the experimentally attained melt (Fig.2 b) [2]. The layers are well defined; layer 1 consisting chiefly of (sub-) angular olivine (Ol) and pyroxene, layer 2 exhibiting acicular Ol set within the interstitial melt. Occasional relict Ol displays secondary overgrowth indicating oscillatory chemical zoning (Fig.3+4b). The forsteritic clasts ($Fa_{\sim 19-22}$) in the lasered specimen are characteristically overgrown by subhedral or euhedral rims that frequently feature inverse zoning towards the host Ol (Fig.3b). Alternating brightness in BSE-SEM images indicates cyclical changes in the Fe/Mg ratio [cf. 2]. Here, overgrowths start with more forsteritic compositions ($Fa_{\sim 13-16}$) than the host Ol and then grade to increasingly fayalitic compositions ($Fa_{\sim 25-41}$); however, normal zoning in Ol was also frequently observed. Pristine urban micrometeorites feature comparable characteristics in phase composition and microtextures (Fig 5+6). A relict forsterite clast (Fa_2) in porphyric sample THMM461 (Fig.6) is surrounded by a more fayalitic rim of anhedral to subhedral, zoned Ol (Fa_{25-42}). Other samples lack any relict clasts and resemble the lasered silicate melts. In these melts, Ol crystals in vicinity of FeNi metal have more fayalitic, but Ni-depleted compositions (Fa_{72-90}; Ni < 0.1 wt%) than the more forsteritic Ol crystals in the metal-poor regions. Locally, skeletal magnetite occurs (Fig.3+4). Original boundaries partly dissolve into melt films coating the Ol grains and trails of intrusions indicate incipient melting (Fig.3+4 c,d). The transition into layer 3 is marked by gradually coarser Ol grain sizes which reflects increasing crystallization of the melt. The latter exhibits a suite of distinctly zoned quench crystals ($Fa_{\sim 15-40}$) with acicular, hopper or tabular shape within the glassy matrix, which displays abundant dendritic or skeletal magnetite crystals, a second generation of olivine nanocrystals(Fig.3+4a), occasional chromite grains, FeNi metal and troilite droplets in spherical to botroidal form (Fig.5). As metal and sulfide typically segregate as immiscible phases, they assemble marginally, if not lost during entry, as observed not only in both experimental and natural fusion crusts but also plentiful in micrometeorites. Preliminary data on FeNi alloys from the experiment indicate Ni-enriched compositions in the irradiated domains suggesting selective oxidation and fractionation of Fe from FeNi metal into the adjacent melt (cf. [8]). Fe oxide rims develop at contact with ambient air during quenching of FeNi metal melts, well agreeing with reports by [5] and [6] and thus corroborating the suitable comparison of thermal histories and redox conditions between natural and experimental fusion crusts.

References

[1] Genge M. J. and Grady M. M. (1999) Meteoritics & Planetary Science 34:341–356. [2] Pittarello L. et al. (2019) Meteoritics & Planetary Science 54:1563–1578. [3] Taylor S. et al. (2000) Meteoritics & Planetary Science 35:651–666. [4] Genge et al. (2008) Meteoritics & Planetary Science 43:497–515. [5] Pittarello et al. (2019) Icarus 331:170–178. [6] Suttle M. D. et al. (2021) Meteoritics & Planetary Science in print. [7] Hamann C. et al. (2018) LPSC XLIX, Abstract #2144. [8] Hamann C. et al. (2013) Geochimica et Cosmochimica Acta 121:291–310.
[9] Genge M. J. et al. (2017) *Geology*, *45*(2): 119-122.

84th Annual Meeting of the Meteoritical Society Chicago

Fraunhofer EMI

The Meteoritical Society

Für Natur MUSEUM FÜR NATURKUNDE BERLIN

Freie Universität Berlin

clarakampf@mfn-berlin.de